Steady State Creep Characteristics of Sn-5wt% Sb-(0.5-3) wt% Ag Solders

M.Sobhy[a,]*, A.M.El-Refai[b]

[a]Physics Department, Faculty of Education, Ain Shams University, P.O. Box 5101, Heliopolis 11771, Roxy, Cairo, Egypt.
[b]Physics Department, Faculty of Women for Art, Science and Education, Ain Shams University, Cairo, Egypt.

The realization of harmful effects of Pb on the atmospheric pollution, environment and human health requires full implementation of new generation of lead-free solders, requires detailed knowledge and understanding of their mechanical behavior. This study reports on structure, thermal and tensile creep properties of Sn–5 wt.%Sb–0.5 wt.%Ag (SSA505), Sn–5 wt.%Sb–1.0 wt.%Ag (SSA510) and Sn–5 wt. %Sb–3.0 wt.%Ag (SSA530) lead-free solder alloys. The obtained results show a surprising desirable decrease in melting temperature with increasing Ag content. Microstructure of the three solder alloys is characterized by the presence of square flat intermetallic compound (IMC) of SbSn particles within β-Sn matrix besides Ag_3Sn IMC. Increasing Ag content led to the increase in size of the Ag_3Sn particles along with an increase in its volume fraction. A remarkable decrease in the size of β-Sn grains is occurred with increasing Ag content. This reduction in size can be attributed to pinning effect of β-Sn grains by Ag_3Sn fine IMC particles. Attention has been paid to the role of IMCs on creep characteristics. In order to relevant the creep characteristics such as stress exponent and activation energy, the tensile creep tests were performed within the temperature range 293–373 K at constant applied stresses. Activation energy (Q) and stress exponent (n) were determined to clarify the deformation mechanism. This study revealed that the solder alloy Sn–5Sb–3.0Ag has potential to give a good and higher creep resistance and lower melting.

1. Introduction

Sn–Pb solder alloys were extensively used as joining materials for assembly and packaging in modern industrial electronic components over recent decades because of its superior performance and low cost [1-3]. Increasing environmental awareness and impending legislation against Pb usage due to its toxic nature development of Pb-free solders and their associated soldering processes owing to many lead-free Sn-based have been developed and their microstructures, mechanical properties and wettability have been reported. Among the developed lead-free solders, those containing Sb and Ag could be of interest because of their suitable mechanical and creep properties [4].

The improved properties have been attributed to the solid solution hardening effects of Sb [5], formation of flat square SnSb particles [6], and the presence of Ag3Sn intermetallics [7] in the Sn matrix. It has also been shown that adding Sb can refine the Ag3Sn precipitate, and thus, improve the mechanical properties and thermal resistance of the Sn–Sb–Ag solders [5]. Binary Sn–Sb alloys belong to a group of potential candidates for high-temperature lead-free solder materials. Their melting temperature can be modified by adding a third element, as for example Ag, Cu or Ni. A lot of studies on Sn–Sb solder alloys have been reported, covering their solidification behavior [8], interfacial reactions on substrates [9], and mechanical properties [10]. El-Daly et al.studied the influence of Ag and Au additions on the physical properties of Sn–Sb solder alloys. Mechanical and thermal property measurements indicated a significant increase in creep resistance and rupture time with the alloying of Ag and Au elements. Chen et al. [11] investigated the interfacial reactions in the Sn– Sb/Ag and Sn–Sb/Cu couples and reported that all the reaction products of IMCs could grow linearly with the square root of reaction time, which suggests that the interfacial reactions are diffusion controlled.

During the process of soldering and subsequent service, solder alloys are supposed to melt and react with substrate to form at least one intermetallic compound (IMC) at the joint interface, and formation and growth of these IMCs can play important roles in affecting the reliability and mechanical and electric properties of the solder joint. If interfacial reaction between solder alloys and substrates can be predicted, it would be helpful to design new multi-component solder alloys and to better understand the physical metallurgy of substrate/solder joint. Moreover, Sn-based alloys are used in some delicate soldering for electronic equipments; they are also used in other fields of industry. More knowledge about their mechanical properties may be helpful in industrial applications. Therefore, this study aims to investigate the effect of Ag content on tensile steady state creep characteristics of the Sn-Sb-xAg solder system.

2. Experimental procedures

Alloys of Sn–5 wt% Sb-0.5 wt% Ag (SSA505), Sn–5 wt% Sb-1.0 wt% Ag (SSA510) and Sn–5 wt% Sb- 3.0 wt % Ag (SSA530) were used in the present study. The three solder alloys were prepared from Sn, Sb and Ag, (purity 99.99) as raw materials and melted in a ceramic crucible at 773K for 1 h. The molten solder in crucible was chill cast in a steel mold to form cylindrical ingots of 10mm in diameter. A cooling rate of 5-8 K/s was achieved, so as to create the fine microstructure typically found in small solder joints in microelectronic packages. The ingots were cold drawn to wire samples of 1×10^{-3} m in diameter and 5×10^{-2} m working length. To obtain samples containing fully precipitated phases, the samples were annealed at 393 K for 1 h, then left to cool slowly to room temperature. Creep tests were performed at 295, 323, 348 and 373K after waiting time of 10 min for each test temperature to be reached. The melting temperature and pasty range of the three solder alloys were analyzed using a differential

scanning calorimeter (DSC) Shimadzu DSC-50. Heating the specimens in DSC was carried out at 10 K/min of heating rate in Ar flow. Microstructure of the as-cast solder alloys was observed by using Optical microscopy (OM), a JEOL scanning electron microscopy (SEM) equipped with energy dispersive X-Ray analysis (EDX) and was analyzed by X-ray diffractmetery (Philips diffractometer (40 kV) with Cu Kα1 radiation (λ = 0.15401 nm) was used for XRD measurements. XRD patterns were recorded in the 2θ range of 20°–90°

3. Results and Discussion

3. 1 Microstructure analysis

To identify the initial phases, the as-cast Sn–Sb-0.5Ag (SSA505), Sn–Sb–1.0Ag (SSA510) and Sn–Sb–3.0Ag (SSA530) experimental alloys were examined by XRD, as shown in Fig.1 (a-c). From this figure it can be seen that all the three as-cast experimental alloys are mainly composed of β –Sn phase, in addition to IMCs SbSn, Ag_3Sn and Ag which appear along with the peaks of β –Sn phase in three alloys. The existence of Ag_3Sn phase in the XRD patterns of all the investigated samples indicate the successful alloying of Sn and Ag after the melting process. In general; the diffraction patterns of three solder alloys SSA505, SSA510 and SSA530 are found to have nearly the same features.

Typical microstructure of the as-cast ternary alloys SSA505, SSA510, SSA530 is shown in Fig. 2a-c. Figure 2a is an optical micrograph (OM) showing bright and dark regions. It can be noticed that the bright regions (β-Sn) is surrounded by dark eutectic mixture (Ag_3Sn/SbSn). Square flat precipitates are observed both in the β-Sn grains and in the eutectic network regions. Such particles had been identified by EDX analysis as SbSn IMCs precipitates. Since Ag has little solubility in β –Sn matrix below 220 ◦C, the eutectic regions become very fine and most of the Ag precipitates as Ag3Sn phase or other forms such as pure Ag (as indicated by XRD in Fig.1). It has been reported previously that Ag_3Sn IMC might act as heterogeneous nucleation sites for β-Sn dendrites upon solidification in SAC solders [12].

EDX analysis (Fig.2f) confirmed that the dark dendrite regions is the β-Sn, Sb and Ag while the bright regions which contain the flat square bright regions are found to contain β-Sn, Sb and Ag. Since the solder used composed of Sn,Sb and Ag, the eutectic mixture contains few flat square SnSb particles and needle-like fine Ag_3Sn particles dispersed within the Sn-rich matrix while the bright regions contain dens flat square bright phase termed as SnSb IMC.

It is not surprising that increasing Ag content from 0.5 to 3 wt% Ag results in increasing concentration of the Ag_3Sn particles along with refined β-Sn grains as well as the SnSb square flat IMC particles (Fig.2 (a-c)). This can be interpreted as follow; the finer Sn-rich grains within higher Ag content solder reveal near-equiaxed grains with homogenous distribution and narrower dendrites shown in Fig. 2(c-d). The decrement of average grain size of the β-Sn phase with increasing

Ag content from 0.5 wt% to 3.0wt% can attribute to the pinning action on grain boundaries and by second phases resulting in limited grain growth **[**13**].** β-Sn phase is not only composed of pure Sn crystals but rather contain several of tiny intermetallic particles that scattered throughout Sn matrix. Furthermore, during solidification of the precipitated particles of Ag3Sn IMC may adsorbed at the surface of the β–Sn grains and surface the square flat SnSb particles. This was in agreement with, Liu et al. [12, 14, and 15] which have found that the adsorption of nano-metric Ag3Sn (IMC) particles occurs during the solidification of SAC. This adsorption decreased the surface energy of the other IMC (Cu6Sn5) and retard the growth of the whole IMC particles. So, the observed reduction in size of the SbSn confirmed by the OM images (Fig. 2(a-c)) can be assigned to the retarding effect of the nano-metric particles Ag3Sn on the growth of SnSb which incorporated into the solder matrix. According to the adsorption theory, increasing the adsorption of elements could decrease the surface energy and/or decrease the growth of IMCs size [16]. For the Sn-Sb-Ag solder, the micro-size of SbSn IMC are larger than the size of the fine needle-like Ag_3Sn particles. Therefore, the incorporation of active surface fine Ag3Sn particles refines the size of SnSb IMC. Previously, similar behavior has been reported [17, 18]. In view of these considerations, it is not surprising to expect increasing stiffness and hardening with increasing Ag content.

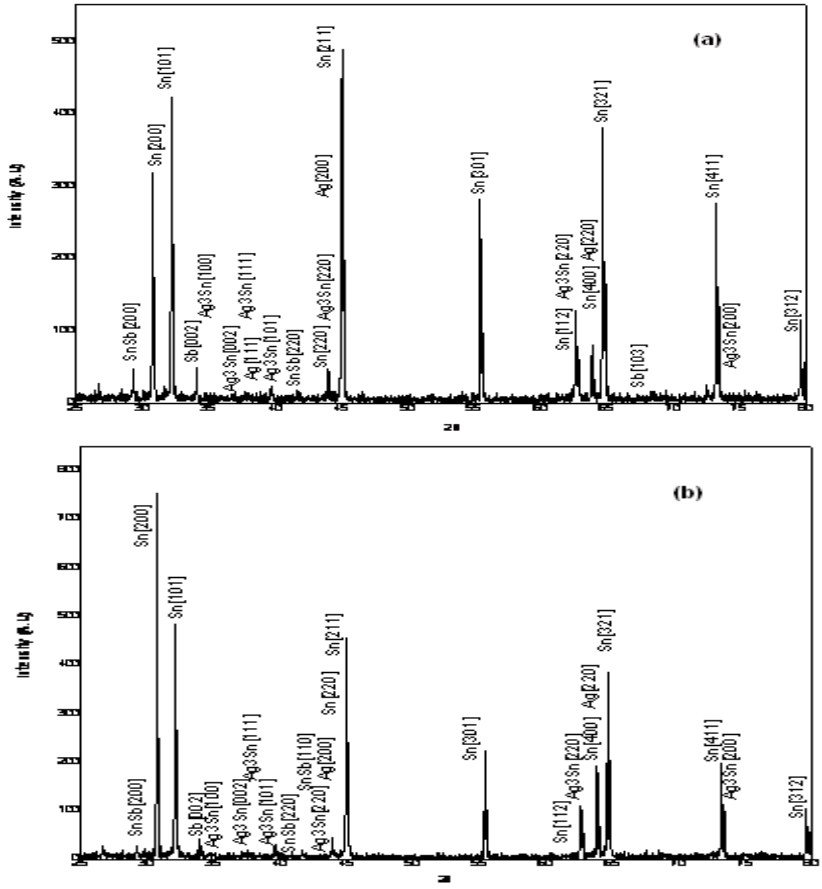

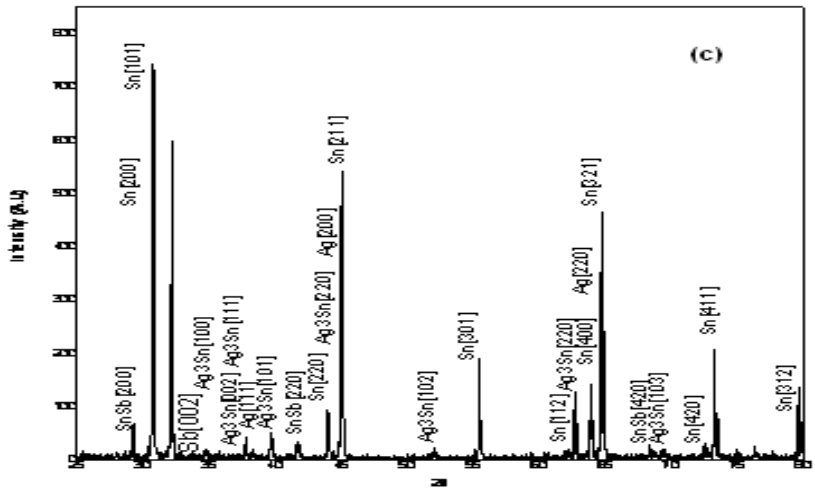

Fig.(1): XRD patterns for: a) SSA505, b) SSA510 and c) SSA530 solder alloys

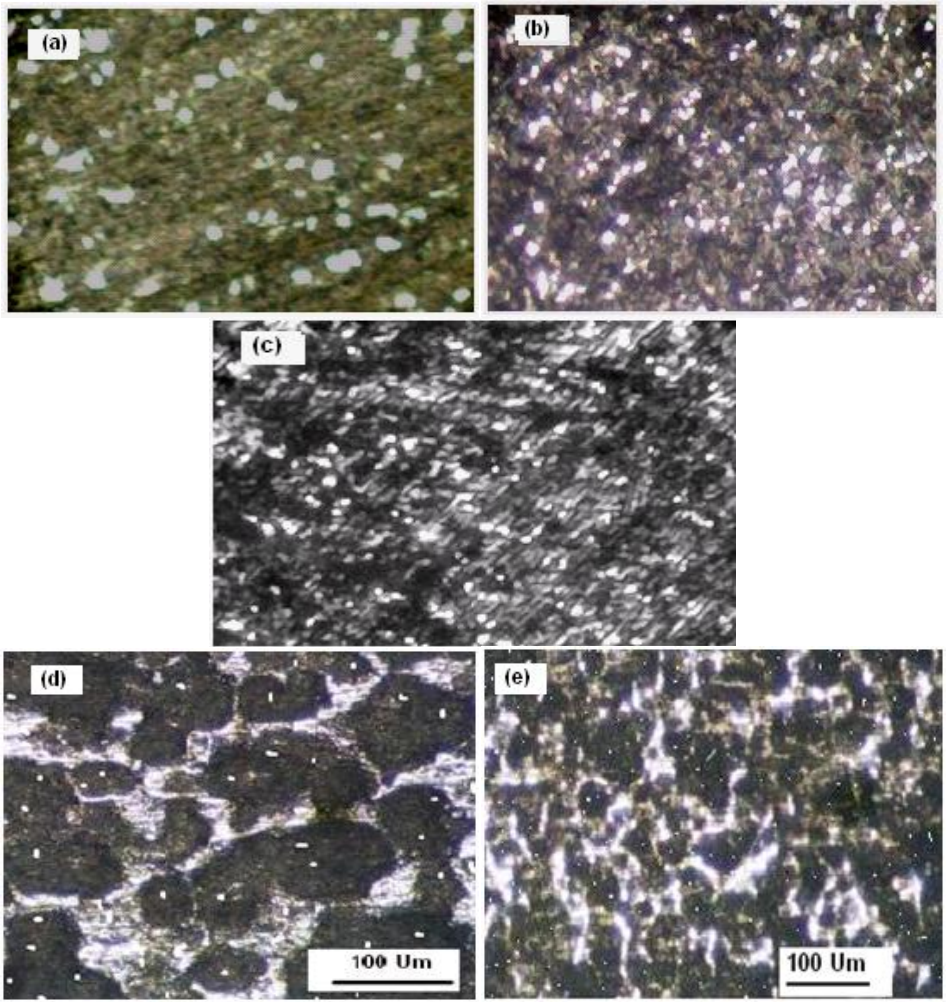

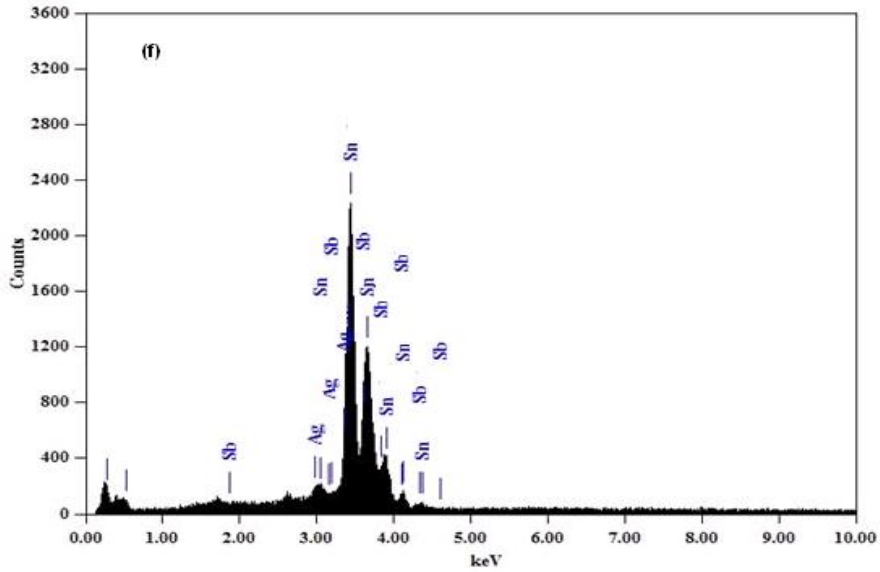

Fig.(2): OM for: a) SSA505. b) SSA510, c) SSA630, d) SEM for SSA505, e) SEM for SSA530 and f) EDX for SSA530 solder alloy

3.2 Thermal Analysis

The melting temperature (Tm) the pasty range (difference between Solidus temperature (TS) and liquidus temperature (Tℓ)) are critical solder characteristics because they determine the maximum operating temperature of the system and the minimum processing temperature which its components must survive. In previous work, DSC analysis at scanning rate of 10 K/min reported that (Ts), (Tm) and (Tℓ) for Sn-5wt%Sb are 240, 246 and 248◦C, respectively [19]. Features of the endothermic peaks of the three solder alloys SSA505, SSA510 and SSA630 are summarized in Table (1). For the three solders there is a significant difference between solidus melting and liquids temperatures Ts, Tm and Tℓ, respectively. Ts, Tm and Tℓ for SSA505 at the endothermic peak are 205.9, 222.5 and 236.6 ◦C, respectively. Increasing concentration of Ag to 3wt% decreased Ts, Tm and Tℓ to 206.8, 218.2 and 232.4 ◦C, respectively, as illustrated in Table (1). It was found also that Tm as well as the pasty range (ΔTℓ - ΔTs) is decreased with increasing concentration of Ag (Fig.3a-b). This result is nearly not verified with other previous studies on SSA solders [20, 21]. It was found similar to that reported by El-Daly et.al [22] on Sn-9Zn solder alloy. They found that adding Bi up to 4wt% decreased Tm of Sn-9Zn from 198.1^{o}C to 194.0^{o}C with slightly expanding in the pasty range. For any alloy to be worthwhile as a solder for electronics industry, it must possess certain specific quantities like melting range or pasty range (difference between solidus and liquidus temperatures) which is an essential parameter to estimate the time required for finishing the soldering process. The pasty range of solder alloys are illustrated in Table (1). The results reflect that, melting temperature of the SSA solder alloys are decreased with increasing Ag content in the investigated range from 0.5 to 3wt%.

Table (1): Thermal characteristic of the investigated solders

Alloy	Ts	Tm	Te	wt% Ag	Pasty range
SSA (105)	205.9	223 .5	236.5	0.5	30.6
SSA (110)	208.2	220.8	234.7	1.0	26.5
SSA (130)	206.8	219.2	232.4	3.0	25.6

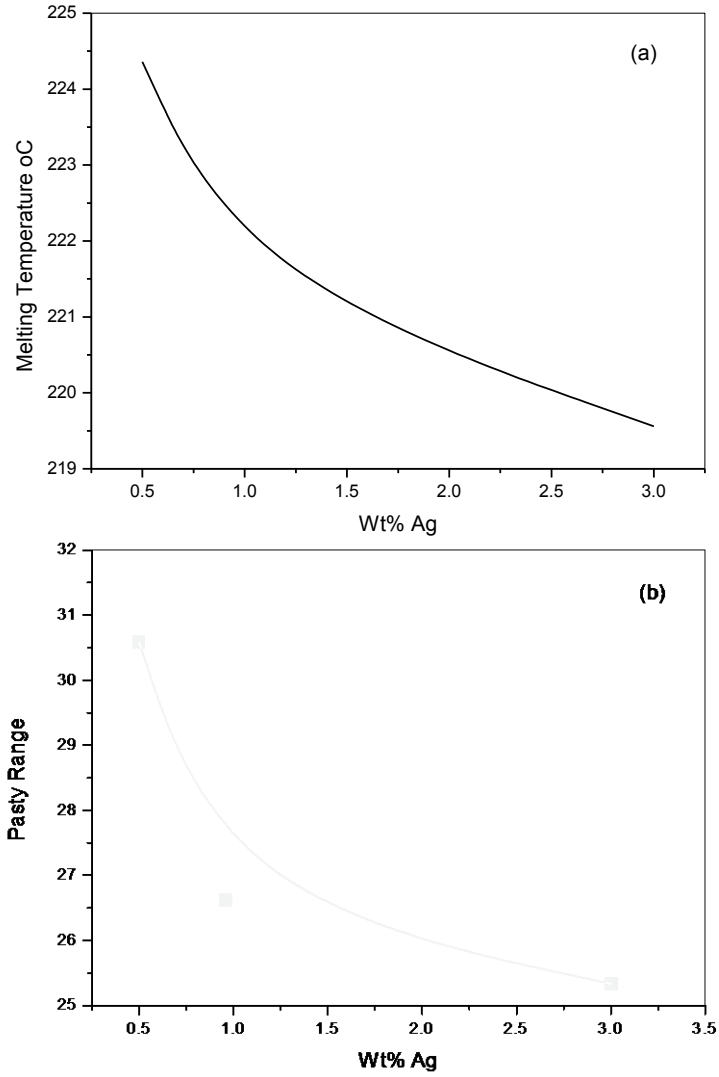

Fig.(3): Dependence of: a) Tm and b) Pasty range (Tℓ - Ts) on the wt% of Ag

4. Creep performance (Features of creep curves)

Tensile creep tests for the three solders Sn–5 wt% Sb - (0.5 -1- 3 wt %) Ag were carried out at the temperatures 295, 323, 348 and 373K under the effect of different applied stresses ranging from 12.73 to 17.83 MPa. Testing temperature, applied stress and Ag percent were found to strongly affect the steady state creep characteristics. Figure 4a shows typical representative creep curves of the SSA505 solder samples tested at different temperatures (295, 323, 348 and 373K) under the effect of constant stress of 17.83MPa. It is obvious from the figure that the creep strain and the minimum strain rate ($\dot{\varepsilon}_{min}$) are monotonically shifted towards higher values with increasing testing temperature. The same behavior was found also with increasing applied stress as has been observed in the representative isothermal creep curves for SSA505 shown in Fig. (4b. & 4c) shows typical isothermal representative creep curves of (SSA) solder samples with different concentrations of Ag [0.5%, 1% and 3.0%Ag]. From this figure, it is apparently clear that increasing Ag content, as expected decreases the creep strain as well as the minimum creep strain rate. Fig 5(a-c) shows the increase in the minimum strain rate ($\dot{\varepsilon}_{min}$) with increasing testing temperatures and/or applied stress but decrease with increasing the concentrations of Ag [0.5%, 1% and 3.0%Ag].

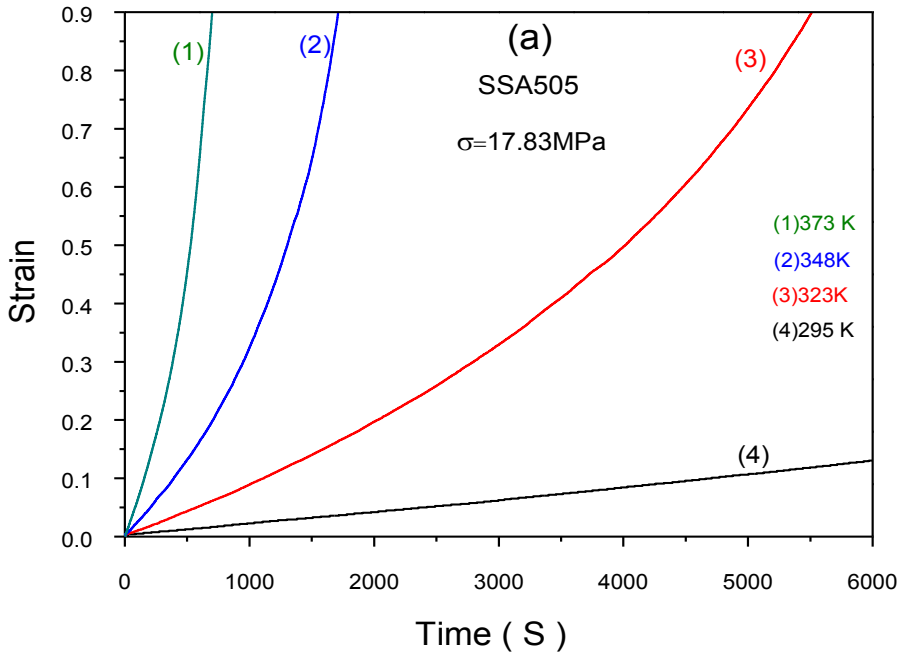

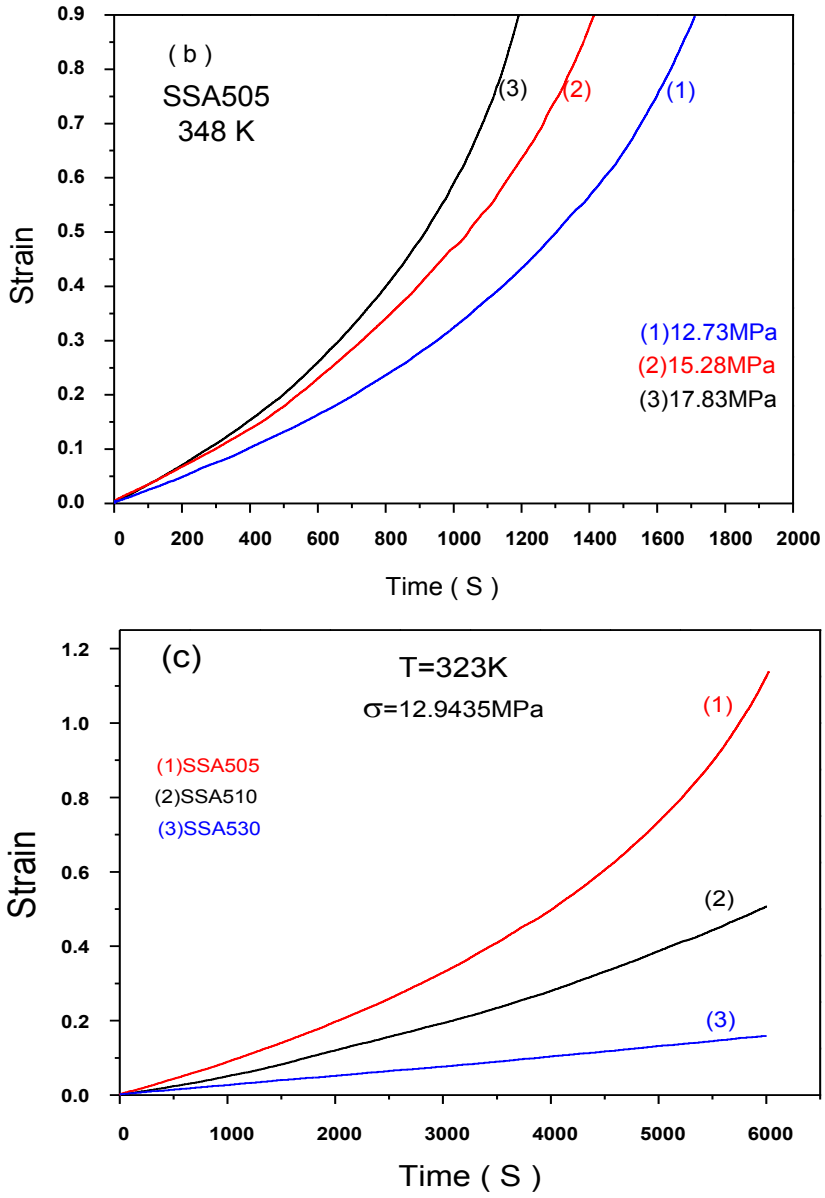

Fig.(4): Representative Strain-time relations showing the effect of: a) Testing temperature on SSA505 under 17.83 MPa, b) different stresses on SSA 505 at a constant testing temperature of 348K and c) SSA with different wt% at 323 under the effect of 12.94MPa

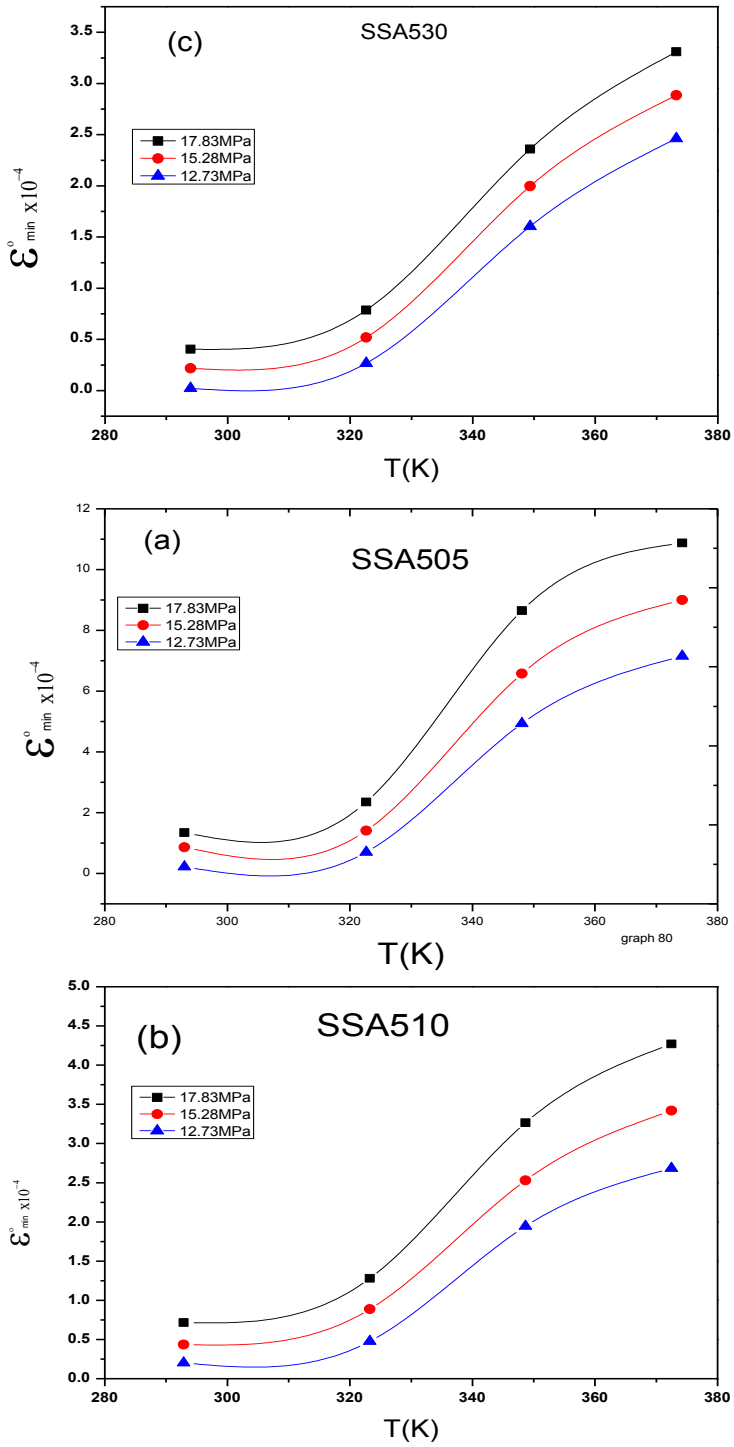

Fig.(5): Relation between min. steady state creep rate and the testing temperatures at different applied stresses as indicated for: a) SSA505, b) SSA510 and c) SSA530.

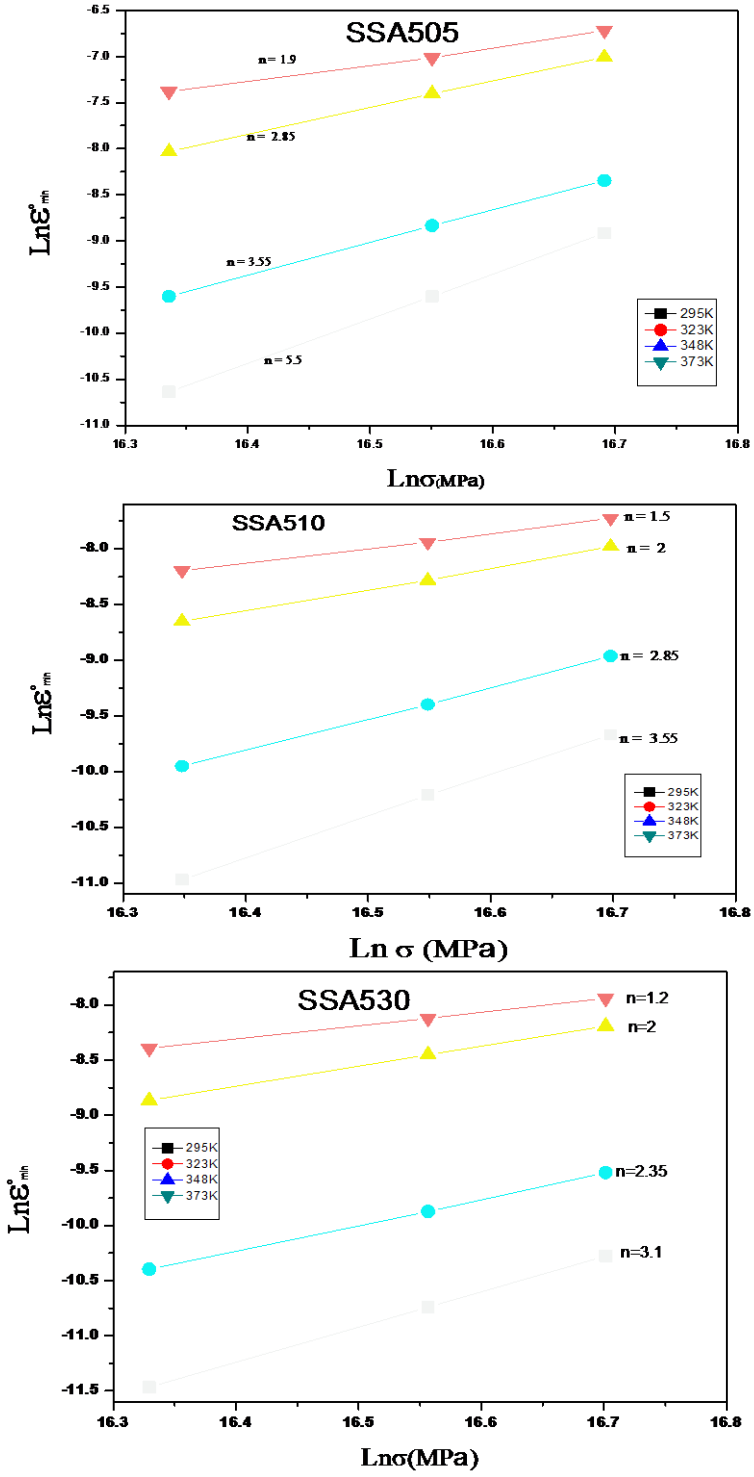

Fig.(6): Ln-Ln relation between min. steady state creep rate and the applied stress at different testing temperatures as indicated for: a) SSA505, b) SSA510 and c) SSA530.

4.1 Stress exponent and activation energy

Results of creep tests conducted at 295, 323, 348 and 373 K over the range of stresses 12.73 -17.83 MPa as representative creep curves are shown in Fig. (4a-c). The minimum creep rate $\dot{\varepsilon}_{min}$ (steady state creep rate) is related to the applied stress, σ, and temperature, T, by the following relation [23]**:**

$$\dot{\varepsilon}_{min} = A\,\sigma^{n} \exp(-Q/RT) \qquad (1)$$

where A is the material-dependent constant and R is the gas constant Q and n are parameters of the material that could give useful information on the creep controlling mechanisms which termed as activation energy and stress exponent, respectively. Stress exponent (n) is obtained from the slopes of the lines relating $\ln\dot{\varepsilon}_{min}$ and ln σ (see Fig. 6a-c). Results of the stress exponent n of the three lead-free solder are listed in Table (2), with values of Q. It is believed that under the experimental test conditions where the Norton power law creep relation is valid, values of n can be related to the mechanisms controlling the deformation process. Table (2) illustrates that the creep stress exponent n of SSA505, SSA510 and SSA530 alloys in the applied temperature range is characterized by an obvious decrease with increasing testing temperature and /or Ag concentration see Fig (7). This means that the stress exponent becomes temperature and Ag concentration dependent for the three solder alloys. It should be emphasized here that such values of n are comparable to that of n values of 6–8.6 at 300–373K for pure tin, 5.5–9.8 at 300–373K for Sn–8.1Sb and 5–7.6 at 296-423K for Sn–3.5Ag, and Sn–5Sb [24-25]. In the obtained results, table 2 shows also that the stress exponents of Sn–5Sb–0.5Ag are relatively high, and about 1.5 times that of the two other alloys SSA510 and SSA530 in the temperature range from 295 to 393 K. However these exponents are typical of dislocation climb-controlled creep [24-26]. In general, the mechanical response and performance of materials change with increasing temperature. Some properties and performance, such as creep resistance decrease with increasing temperature. The reported simple Arrhenius type relationship (equation 1) is used to determine the energy required for activating creep process. It was calculated from the slopes of the lines relating $\ln\dot{\varepsilon}_{min}$ &1000/T (Fig. 8a-c). Values of the activation energy are listed in Table (2) for the three solder alloys. It was found to be dependent on the Ag content and the applied stress see Fig. (9). A review of literature on creep mechanisms in tin-based alloys showed significant discrepancy in the n values and Q values due to the high degree of anisotropy in tetragonal Sn. Mohamed et al. [27] obtained n = 6.6 and Q= 96 kJ/mol from creep tests up to 475K, and these were attributed to a dislocation climb mechanism. It has been reported also that the dislocation climb through obstacles of Sn–5Sb and Sn–5Sb–3.5Ag, may led to values of n = 5.4 and Q= 53.8 kJ/mol, at low stress levels, and n = 11.4 and Q= 75.8 kJ/mol at high stress levels [28]. However these values are in somehow agreement with n (5.5-1.2) and Q (0.26 – 0.57eV) obtained for Sn-5Sb-(0.5-3)% Ag solders alloys in the present work which can suggest that the dominant creep mechanism observed for Sn-based alloys deform by dislocation climb [29]. This result also indicates that the energy barrier for creep

in Ag-containing solder is raised and the dislocation motion is hindered to a greater extent by the hard Ag_3Sn/SnSb IMCs in this alloy. The fact that creep resistance of Sn–5Sb–3.0Ag is better than that of the Sn–5Sb alloy makes the dispersion-hardening approach is promising for the development of convenient alternatives to the high melting point Sn–5Sb-3.0Ag solder alloy.

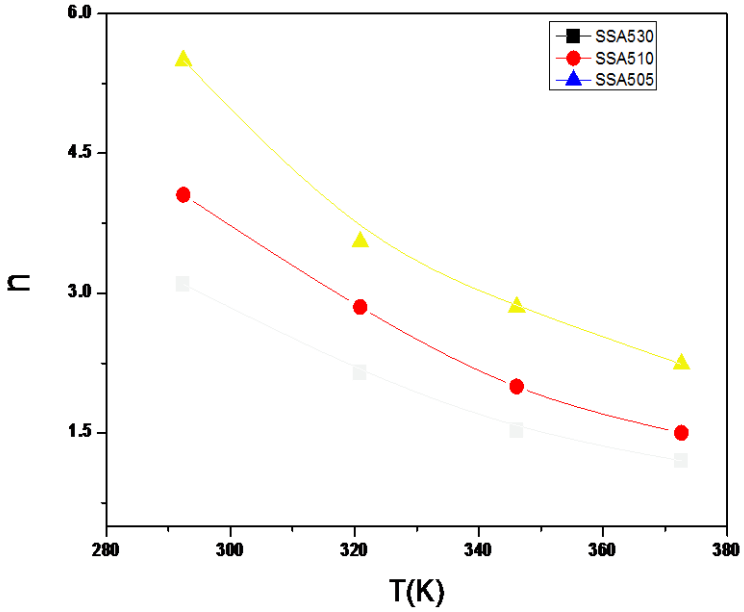

Fig.(7): Dependence of exponent n on testing temperatures or different concentrations of Ag as indicated.

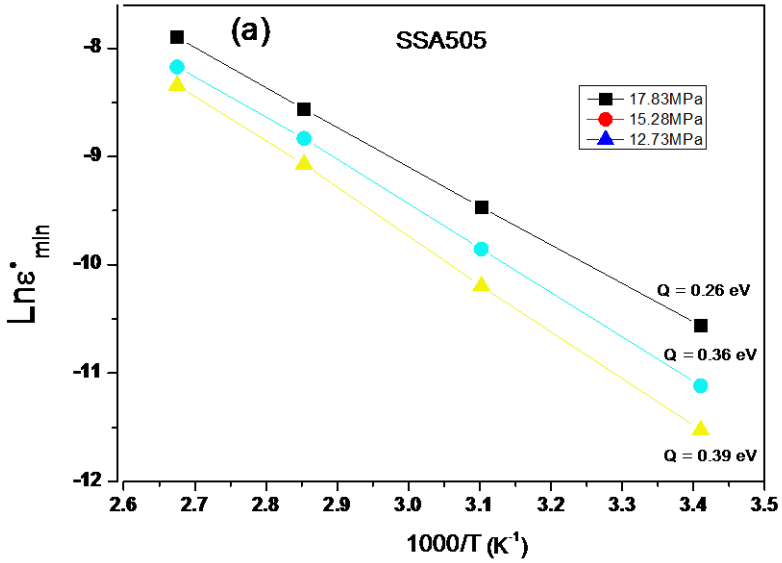

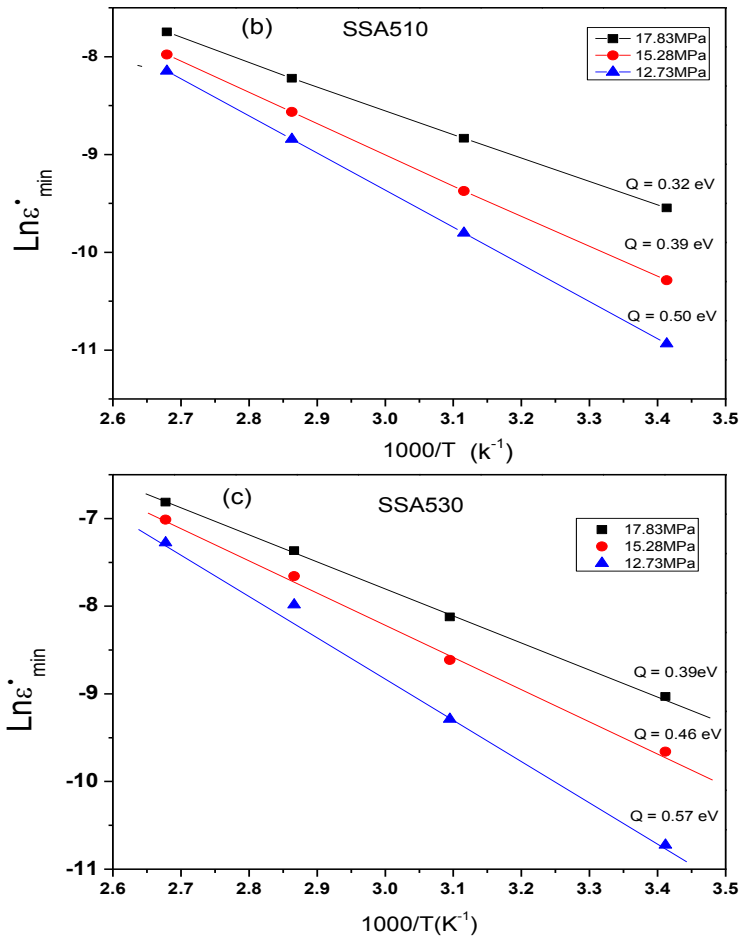

Fig.(8): Relation between ln $\dot{\varepsilon}_{min}$ and 1000/T(K^{-1}) at different applied stresses as indicated for: a) SSA505, b) SSA510 and c) SSA530

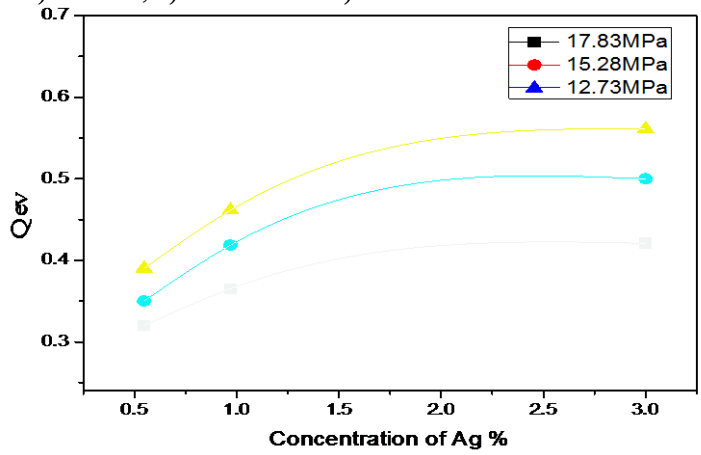

Fig.(9): Dependence of activation energy on the different concentrations of Ag for different applied stress as indicated.

Table (2): Activation energy (Q) and stress exponent (n) values for SSA505, SSA510 and SSA530 solder alloys.

Alloy	E (eV)	σ (MPa)	Testing Temperature (K)	n
SSA (505)	0.26	17.83	295	5.5
	0.35	15.28	323	3.55
	0.39	12.73	343	2.85
	-----	------	373	1.9
SSA (510)	0.32	17.83	295	3.55
	0.39	15.28	323	2.85
	0.50	12.73	343	2.25
	------	------	373	1.5
SSA (530)	0.39	17.83	295	3.1
	0.46	15.28	323	2.35
	0.57	12.73	343	1.85
	------	------	373	1.2

Conclusions

Creep strain tests were conducted on SSA505, SSA510 and SSA530 of solder alloys in the temperature range 293 to 393K under effect of stresses ranged from *** to *** MPa. The temperature and stress dependence were investigated in order to grasp the essential creep deformation behavior of the solder bulk material. The findings in this paper are shown as follow:

1- Melting point of Sn-5Sb-xAg decreased with increasing Ag content
2- XRD and EDX analysis reflect the presence of SbSn, Ag3Sn IMCs
3- A detectable improvement in the steady state creep resistance with increasing Ag content.
4- The dominant creep deformation mechanism observed is the dislocation climb.
5- The energy barrier for creep in Ag-containing solder is raised and the dislocation motion is hindered to a greater extent by the hard Ag3Sn/SnSb IMCs in this alloy

References

1. D.A. Shnawah, S.B.M. Said, M.F.M. Sabri, I.A. Badruddin, F.X. Che, *J. Electron. Mater*., **41**, 2631 (2012).
2. F.X. Che, J.H.L. Pang, *J. Alloys Comp*., **541**, 6 (2012).
3. Q.V. Bui, S.B. Jung, *J. Alloys Comp*., **560**, 54 (2013).
4. M. Kangooie, R. Mahmudi, A.R. Geranmayeh, *J. Electron. Mater*., **39**, 215 (2010).
5. H.T. Lee, H.S. Lin, C.S. Lee, P.W. Chen, *Mater., Sci., Eng*., A **407**, 36 (2005).
6. R. Mahmudi, A.R. Geranmayeh, M. Bakherad, M. Allami, *Mater., Sci., Eng*., A **457**, 173 (2007).

7. H. Rhee, K.N. Subramanian, A. Lee, G. Lee, *Solder. Surf. Mount Technol*. **15**, 21 (2003).

8. SW Chen, CC Chen, Gierlotka W, Zi AR, Chen PY, Wu HJ. Phase equilibria of the Sn–Sb binary system. *J. Electron Mater*, **37**, 992 (2008).

9. CY Lin, C Lee, X Liu, YW Yen. Phase equilibria of the Sn–Sb–Ag ternary system and interfacial reactions at the Sn–Sb/Ag joints at 400oC and 150oC. Intermetallics, **16**, 230 (2008).

10. El-Daly AA, Mohamad AZ, Fawzy A, El-Taher A.M. *Mater. Sci. Eng*., A **528**, 1055 (2011).

11. Guang Zeng, Stuart McDonald, Kazuhiro Nogita, *Microelectronics Reliability*, **52**, 1306 (2012).

12. A. Fawzy, S. A. Fayek, M. Sobhy, E. Nassr , M. M. Mousa, G. Saad, *Materials Science and Engineering* A **603**, 1 (2014).

13. M. E. Alam, S. M. L. Nai and M. Gupta, *J. Alloys Comp*., **476**, 199 (2009).

14. P. Liu, P. Yao, J. Liu, *J. Electron. Mater*, **37**, 874 (2008) .

15. S.Y. Chang, C.C. Jain, T.H. Chuang, L.P. Feng, L.C. *Tsao, Materials & Design*, **32**, 4720 (2011).

16. A.A.El-Daly, A.Fawzy, S.F.Mansour, M.J.Younis, *Materials Science & Engineering* A **578**, 62 (2013).

17. F. Tai, Fu Guo, Zhi-dong Xia, Yong-ping Lei, Yao-wu Shi, International Journal of Minerals, *Metallurgy and Materials*, **16**,6, 677 (2009),

18. Y. W.Shi, P. J. Liu, Y. F. Yan, Z. D. Xia, Y. P. Lei, F. Guo, *J. Electron Mater*, **37**, 507 (2008).

19. A.A.,El-Daly, A. Fawzy, Mohamad, A.Z., El-Taher, A.M. *Journal of Alloys and Compounds*, **509**, 4574 (2011).

20. P. Babaghorbani, S. M. L. Nai, M. Gupta, *Journal of Material Science, Mater Electron*, **20**, 571 (2009).

21. A. Haseeb, M. M. Arafat, M. R. Johan, *Journal of Materials Characterization*, **64**, 27 (2012).

22. A. A. El-Daly, Y.Swilem, M. H. Makled, M. G. El-Shaarawy, and A.M. Abdraboh, *J. Alloys Comp*, **484**, 134 (2009).

23. A.A. El-Daly, *Phys. Stat. Sol*., A **201**, 2035 (2004).

24. S. Choi, J. Lee, F. Guo, T. Bieler, K. Subramanian, *J. Lucas, JOM* 53, 22 (2001).

25. M. Huang, C.Wu, L.Wang, *J. Electron. Mater*., **34**, 1373 (2005).

26. M. Kerr, N. Chawla, *JOM* **65**, 50 (2004).

27. F. Mohamed, K. Murty, J. Morris, *Metall. Mater. Trans*., **4**. 935 (1973).

28. E.A. Brandes, G.B. Brook (Eds.), Smithell's Metals Reference Book, 7th edition,Butter worth-Heinemann, 77 (1992).

29. H. Song, J. Morris Jr., F. Hua, *Mater. Trans*., **43**, 1847 (2002).